



Diffraction moiré fringes as analysis and alignment tools for multilayer fabrication in soft lithography

Jae-Hwang Lee, Chang-Hwan Kim, Yong-Sung Kim, Kai-Ming Ho, Kristen Constant, Wai Leung, and Cha-Hwan Oh

Citation: *Applied Physics Letters* **86**, 204101 (2005); doi: 10.1063/1.1927268

View online: <http://dx.doi.org/10.1063/1.1927268>

View Table of Contents: <http://scitation.aip.org/content/aip/journal/apl/86/20?ver=pdfcov>

Published by the [AIP Publishing](#)

Articles you may be interested in

[Strained hetero interfaces in Si/SiGe/SiGe/SiGe multi-layers studied by scanning moiré fringe imaging](#)

J. Appl. Phys. **114**, 053518 (2013); 10.1063/1.4817729

[Thermomechanical noise measurement of polydimethylsiloxane microcantilevers fabricated by multilayer soft lithography](#)

AIP Advances **3**, 032103 (2013); 10.1063/1.4794692

[Analysis of moiré fringes by Wiener filtering: An extension to the Fourier method](#)

AIP Conf. Proc. **1466**, 155 (2012); 10.1063/1.4742285

[Characterization of field stitching in electron-beam lithography using moiré metrology](#)

J. Vac. Sci. Technol. B **18**, 3287 (2000); 10.1116/1.1313573

[Quantifying distortions in soft lithography](#)

J. Vac. Sci. Technol. B **16**, 88 (1998); 10.1116/1.589841

MULTIPHYSICS SIMULATION
Modeling and App Design Stories

UNIVERSITY • INTEL • ABB SEMICONDUCTORS • ROCH
RS • WITRICITY • MEDTRONIC • PURDUE UNIVERSITY • IN
M DIMATIX • CYPRESS SEMICONDUCTORS • WITRICITY
CTORS • ROCHE DIAGNOSTICS • FUJIFILM DIMATI
RDUE UNIVERSITY • INTEL • ABB SEMICONDUCTO
NDUCTORS • WITRICITY • MEDTRONIC • PURDUE U

COMSOL

READ LATEST ISSUE »

The advertisement features a dark background with a car's front end on the right. On the left, there is a green shield icon with a white lightning bolt. Two small inset images show simulation results: one with a color-coded stress or temperature distribution on a mechanical part, and another showing a blue and yellow flow or field distribution. The text 'MULTIPHYSICS SIMULATION' is in large, bold, white letters, with 'Modeling and App Design Stories' below it. A list of company names is partially visible in the background. The COMSOL logo is at the bottom left, and a blue button with white text 'READ LATEST ISSUE »' is at the bottom right.

Diffracted moiré fringes as analysis and alignment tools for multilayer fabrication in soft lithography

Jae-Hwang Lee, Chang-Hwan Kim, Yong-Sung Kim, and Kai-Ming Ho^{a)}

Ames Laboratory-U.S. DOE and Department of Physics and Astronomy, Iowa State University, Ames, Iowa 50011

Kristen Constant

Department of Materials Science and Engineering, Iowa State University, Ames, Iowa 50011

Wai Leung

Microelectronics Research Center and Ames Laboratory U.S. DOE, Iowa State University, Ames, Iowa 50011

Cha-Hwan Oh

Department of Physics, Hanyang University, Seoul 133-791, South Korea

(Received 21 January 2005; accepted 28 March 2005; published online 9 May 2005)

We studied the first-order diffracted moiré fringes of transparent multilayered structures comprised of irregularly deformed periodic patterns. By a comparison study of the diffracted moiré fringe pattern and detailed microscopy of the structure, we show that the diffracted moiré fringe can be used as a nondestructive tool to analyze the alignment of multilayered structures. We demonstrate the alignment method for the case of layer-by-layer microstructures using soft lithography. The alignment method yields high contrast of fringes even when the materials being aligned have very weak contrasts. The imaging method of diffracted moiré fringes is a versatile visual tool for the microfabrication of transparent deformable microstructures in layer-by-layer fashion. © 2005 American Institute of Physics. [DOI: 10.1063/1.1927268]

Soft lithography has attracted the attention of researchers over the past few years because of its versatile capabilities for generating patterned structures.¹ The growing demand for patterned multilayer structures²⁻⁵ will require more accurate and reliable alignment methods for soft lithography. Since alignment techniques are very critical in layer-by-layer fabrication of multilayered devices, various techniques based on alignment markers are used in semiconductor processing.^{6,7} In soft lithography, however, elastomeric stamps and molds replace photomasks in conventional lithography. In general, the main drawback to using elastomeric materials, such as poly dimethylsiloxane (PDMS), is distortion by stress, due to contraction on curing of the elastomers and contact with a substrate. Although rigid back planes have been introduced to elastomeric stamps to suppress the distortion,^{8,9} it is not clear that they can be used for all applications. For example, the flexibility of the mold is required to facilitate release of transferred structures in microtransfer molding (μ TM).¹⁰ Consequently, we need to monitor the whole sample area for the multilayer alignment if there is substantial pattern distortion.

In this letter, we present a simple and versatile free-space moiré fringe-based scheme for vertically integrated optically transparent structures, for example, in the case of layer-by-layer fabrication using soft lithography. Metrologies based on moiré fringes have been widely used as diagnostic tools for stress-strain analysis,^{11,12} because of their high sensitivity to spatial displacements. We will study the use of the zeroth- and the first-order diffracted moiré fringes (zeroth- and first-DMFs) to visualize the alignment of multilayered three-dimensional (3D) grating structures. We found that DMFs

offer a nondestructive way to obtain structural information. Furthermore, the use of higher-order fringes can help to clarify complex irregular moiré fringes effectively during an alignment in 3D multilayer microfabrication.

To image moiré fringes, we used the two configurations shown in Figs. 1(a) and 1(b) since the whole imaging area can be placed at the same working distance. The dotted arrows in Fig. 1 represent the first-order diffraction angle for a certain wavelength. However, the beams emerging at this angle comprise mainly two different diffracted beams, the zeroth-order at the lower grating and the first order at the upper grating and vice versa. We will simply call the moiré fringe imaged at this angle the first-DMF. A white-light source is positioned at a selected angle, and a microscope objective lens (achromatic plan 4 \times , numerical aperture = 0.17) with a 0.66 in. complementary metal-oxide-semiconductor camera is placed normal to the sample plane. A circular aperture of 3 mm diameter was mounted in front of a condenser lens to increase depth of field. The distance between the aperture of the illuminator and the sample plane

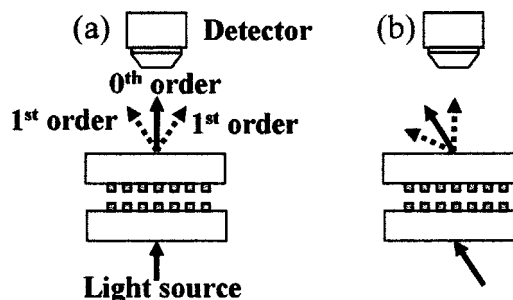


FIG. 1. Schematic illustration of configurations for (a) zeroth-DMF and (b) first-DMF imaging.

^{a)}Electronic mail: kmh@ameslab.gov

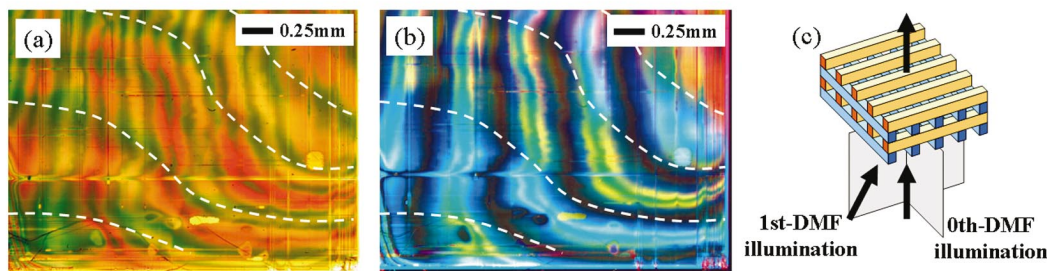


FIG. 2. (Color) Moiré fringes of a four-layered grating structure monitored by (a) zeroth-DMF and (b) first-DMF with (c) their imaging configuration. The white dashed lines represent boundaries of color domains in the first-DMF.

was about 120 mm. By choosing an illumination angle as the first-order diffraction angle of green light ($\lambda=550$ nm), first-order diffracted beams for most visible light can be monitored with the imaging system when using gratings having a periodicity of $2.5 \mu\text{m}$.

We prepared a transparent four-layer polymer grating structure on a glass substrate using μTM . The bars of each grating layer were $1.4 \mu\text{m}$ wide and $1.1 \mu\text{m}$ high, and the orientation of each layer was perpendicular to that of the neighboring layers. Figure 2 shows the moiré patterns of the four-layer grating structure using the two different configurations depicted in Figs. 1(a) and 1(b). The zeroth-DMF in Fig. 2(a) shows more complex features than that of first-DMF in Fig. 2(b) since the zeroth-order beam carries all alignment information for both independent orientations of gratings without discrimination, and one period of the fringes is composed of similar subperiods. Moreover, the higher background signal due to the bright field may reduce the signal-to-noise ratio in imaging when superimposing optically transparent patterns.

In contrast, the first-DMF in Fig. 2(b) clearly shows the moiré fringe formed by a pair of gratings in which bars are aligned perpendicular to illumination angle. In addition to the selective visualization as the grating layers are aligned, the first-DMF is much more distinct than the zeroth-DMF by virtue of high contrast in fringe formation. This enhanced contrast is due to dark fringes, not observed in the zeroth-DMF. The multicolor feature in DMFs originates mainly from the dispersive nature of the gratings. This dispersive first-DMF seems effective for the visual analysis of irregular moiré fringes. For example, the first-DMF in Fig. 2(b) has several color domains, and the domains coincide with the moiré fringe of the second and fourth grating layers as seen in Fig. 2(a). By this correlation, we can get the information of the other orientation without deteriorating the contrast of the first-DMF of the first and third grating layers. Note that several straight lines in both optical images in Fig. 2 are defect sites where some pattern bars are missing from errors in fabrication. Since these linear defects show the actual orientation of the grating structures in the DMFs, we can see that the orientation of the irregular moiré fringe is altered dramatically, while the orientation of actual bars did not change much.

Knowing the correspondence between a multilayer structure and its moiré fringes allows us to develop a simple non-destructive evaluation method. We performed a comparison mapping study between the moiré fringes and the real structure based on scanning electron microscopy (SEM). After cutting a four-layer grating structure at 45° to the orienta-

tions of each layer to observe a cross section, we compared the first-DMFs with SEM micrographs as shown in Fig. 3. From the mapping, we can see that the dark fringes in the first-DMF appear when the bars in the third layer are positioned in the middle of a gap between the bars in the first layer. According to the calculation of Yamamoto *et al.*,¹³ when two identical gratings are aligned in the same direction, the intensity of the first-order diffraction is minimized, as phases of the gratings are opposite.¹³ The dark fringe in the first-DMF can be interpreted in a similar manner. The dark fringe enhances the contrast of the first-DMF and serves as a reliable marker showing alignment information.

An alignment technique for the soft lithography should be able to align patterns under various situations, even when the contrast of patterns is insufficient. For example, a transparent PDMS mold used in μTM may carry transparent polymers within its patterned channels. The moiré fringes become significantly fainter after the channels are filled with a polymer to be transferred if the refractive index of the filled polymer is close to that of the PDMS mold. In multilayer fabrication, the recognition of the faint moiré fringes may be difficult in the background of pre-existing moiré fringes from previously stacked structures.

To show the feasibility of this moiré alignment scheme based on the first-DMFs, we tried an alignment of a three-layer grating structure on a glass substrate and a patterned PDMS mold whose channels are filled with a polymer. The experimental schemes are shown in Fig. 4(c). The refractive indices of cured PDMS (Sylgard 184, Dow Corning) and the filled polymer (J-91, Summers Optical) are 1.43 (Ref. 14) and 1.55 (Ref. 15) in visible ranges, respectively. As a result of the filling, the contrast of the PDMS pattern, $\Delta n/n_{\text{PDMS}}$, is significantly decreased from 30% to 7%, where n_{PDMS} and Δn are the refractive index of cured PDMS and the difference of the indices of PDMS and filled material, respectively.

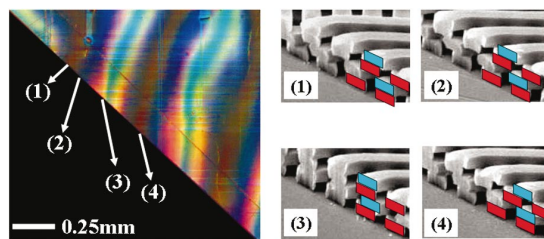


FIG. 3. (Color) Mapping of first-DMFs, generated by the first and third layer of a four-layered grating structure, to their corresponding SEM micrographs is shown. The first and third layers, and the second and fourth layers are colored red and blue, respectively, in the SEM micrographs.

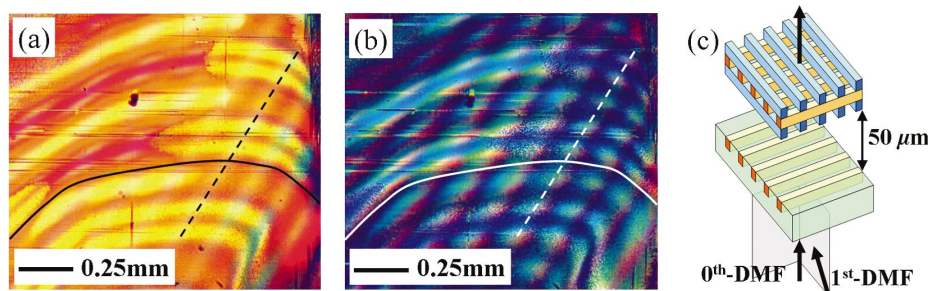


FIG. 4. (Color) (a) zeroth-DMF and (b) first-DMF in alignment are shown with (c) their imaging configuration. The solid and dashed lines are inserted in both images along preformed and newly formed fringes, respectively.

First, the upper three-layer structure was focused, and then the lower polymer-filled PDMS was raised to the upper structure. In the case of the first-DMF, the angle of illumination was perpendicular only to the orientation of the second layer and the PDMS mold to suppress the moiré fringe from the first and third layers. The images of both zeroth- and first-DMFs are shown in Figs. 4(a) and 4(b), respectively, when the PDMS mold was apart from the three-layer structure about $50\ \mu\text{m}$. Although the absolute brightness of the zeroth-DMF is higher than first-DMF's, the brightness, not contrast, was adjusted to have a similar level automatically. The first-DMF was clearly visible at a separation from around $300\ \mu\text{m}$ and the contrast increased as the separation decreases. The large proximity gap gives sufficient room for relative movement for sample alignment before contact. As shown in Fig. 4(a), the preformed moiré fringe by the first and third layer is more distinct than that of the newly formed moiré fringe by the second layer and the polymer-filled PDMS mold. The faintness is because of the low contrast of the pattern on the PDMS mold due to the polymer filling and the PDMS mold not being in exact focus. Under the same conditions, the faint fringe in Fig. 4(a) became significantly clearer in the first-DMF shown in Fig. 4(b) and comparable to the preformed moiré fringe. Although the preformed moiré was not suppressed entirely, the enhanced contrast facilitates alignment in layer-by-layer fabrication.

In conclusion, we demonstrated a visual alignment system for layer-by-layer microfabrication based on diffracted moiré fringes with white light. The comparison study between the moiré pattern and SEM cross section micrograms demonstrated that DMFs can be used as a noninvasive optical inspection tool for obtaining structural information of multilayer samples. The imaging of first-DMF has a number of attractive features for analysis and alignment of multilayer microstructures: Selective imaging depending on aligned orientation; enhanced contrast of moiré fringes; availability of a visual inspection of alignment status; and simplicity in the

multilayer alignment even under low contrast of patterns. With these advantages, the imaging method of the first-DMF should be applicable for 3D fabrication of microstructures using soft lithography, as an inspection and alignment tool even when moiré patterns are extremely complex.

This work is supported by the Director for Energy Research, Office of Basic Energy Sciences. The Ames Laboratory is operated for the U. S. Department of Energy by Iowa State University under Contract No. W-7405-ENG-82. One of the authors (C.H.O.) thanks the Korea Science and Engineering Foundation through the quantum photonic Science Research Center for financial support.

- ¹Y. Xia and G. M. Whitesides, *Angew. Chem., Int. Ed. Engl.* **37**, 550 (1998).
- ²S. Y. Lin, J. G. Fleming, D. L. Hetherington, B. K. Smith, R. Biswas, K. M. Ho, M. M. Sigalas, W. Zubrzycki, S. R. Kurtz, and Jim Bur, *Nature (London)* **394**, 251 (1998).
- ³M. A. Burns, B. N. Johnson, S. N. Brahmasandra, K. Handique, J. R. Webster, M. Krishnan, T. S. Sammarco, P. M. Man, D. Jones, D. Heldsinger, C. H. Mastrangelo, and D. T. Burke, *Science* **282**, 484 (1998).
- ⁴J. Park and P. T. Hammond, *Adv. Mater. (Weinheim, Ger.)* **16**, 520 (2004).
- ⁵T. Thorsen, S. J. Maerkl, and S. R. Quake, *Science* **298**, 580 (2002).
- ⁶T. Nomura, S. Kimura, Y. Uchida, and S. Hattori, *J. Vac. Sci. Technol. B* **6**, 394 (1988).
- ⁷H. Zhou, M. Feldman, and R. Bass, *J. Vac. Sci. Technol. B* **12**, 3261 (1994).
- ⁸J. A. Rogers, K. E. Paul, and G. M. Whitesides, *J. Vac. Sci. Technol. B* **16**, 88 (1998).
- ⁹H. Schmid and B. Michel, *Macromolecules* **33**, 3042 (2000).
- ¹⁰X. M. Zhao, Y. Xia, and G. M. Whitesides, *Adv. Mater. (Weinheim, Ger.)* **8**, 837 (1996).
- ¹¹O. Kafri and I. Glatt, *The Physics of Moiré Metrology* (Wiley-Interscience, New York, 1990), Chap. 5.
- ¹²B. Han, in *Handbook of Moiré Measurement*, edited by C. A. Walker (Institute of Physics, Bristol, 2004), Chap. 2, pp. 18–24.
- ¹³N. Yamamoto and S. Noda, *Jpn. J. Appl. Phys., Part 1* **37**, 3334 (1998).
- ¹⁴Publication No. 10-042D-98, Dow Corning, Midland, MI.
- ¹⁵The value of the refractive index was acquired from Summers Optical (www.emsdiasum.com).